## Subtraction-based densities for positrons created inside supercritical fields

C. Gong, 1,2 O. Su , 2 and R. Grobe<sup>2</sup>

<sup>1</sup>Department of Mathematics and Physics, North China Electric Power University, Baoding 071003, China <sup>2</sup>Intense Laser Physics Theory Unit and Department of Physics, Illinois State University, Normal, Illinois 61790-4560, USA

9

10

11

12

15

16

17

19

20

21

23

29

31

33

35

42

50

We introduce an approach to investigate the spatial distribution of positrons generated from the Dirac vacuum state through a localized supercritical electric field. The well-known degeneracy of energy states in the upper and lower continua of a supercritical Dirac Hamiltonian has posed a significant challenge in distinguishing between the appropriate subspaces of electronic and positronic states within the interaction zone. Consequently, accurately partitioning the fully coupled quantum field operator into its electronic and positronic contributions has been widely viewed as problematic. However, this partitioning would be beneficial for determining positronic densities, which would provide valuable insights into the particles' birth positions and production rate within the interaction zone. Naturally, the computed quasidensities obtained by projecting onto force-free (or partially dressed) energy eigenstates exhibit spatially dependent mathematical corrections, resulting in deviations from the true physical positronic density. These corrections are not attributable to real particles during the interaction. Our work focuses on developing a quantitative understanding of these corrections, allowing us to effectively subtract them out and gain insights into the genuine dynamics within the pair-creation interaction zone.

### DOI: 10.1103/PhysRevA.00.003100

### I. INTRODUCTION

One of the most intriguing predictions of strong-field quantum electrodynamics is the prospect that elementary particles, such as electrons and positrons, can emerge from the vacuum's quantum state under the influence of extraordinarily powerful external fields [1–6]. Despite the significance of this phenomenon, it is remarkable that the fundamental mechanisms underlying the birth of matter in such a scenario, within the full context of space-time, remain far from being comprehended. This enigma gives rise to a multitude of questions, each pivotal in its own right: Where precisely within the localized external field region do positrons come into existence? Do positrons and electrons within a pair materialize at the same location, or do they exhibit a certain separation? Is the birth of positrons and electrons synchronized, as suggested by classical conservation of total charge? Are these particles born at rest, or is there an inherent velocity distribution? And, what about the interrelated characteristics of particles within a pairdo they adhere to intuitive classical mechanics expectations?

The absence of answers to these questions largely stems from the well-established challenge of formulating the fundamental laws or theoretical framework necessary to describe the dynamics at the point of particle generation. Presently, even distinguishing between positrons and electrons within the interaction zone presents a formidable challenge. However, a clever theoretical approach circumvents this dilemma by focusing solely on predicting particle properties after they have exited the interaction zone. In this S-matrix based method [7–9], the interaction zone is treated as a black box environment.

Lessons from other realms of physics, such as the study of strong-field ionization in atoms and molecules, underscore the immense value of gaining microscopic insights into electronic dynamics [10]. Theoretical investigations with a comprehensive space-time resolution have unveiled various mechanisms, leading to phenomena like the generation of higher harmonics in scattered light spectra [11,12], above-threshold ionization [13], and atomic stabilization [14]. There is no inherent reason why quantum field theoretical studies of pair creation could not benefit from a similar level of advancement.

54

55

57

58

61

62

65

69

70

71

72

74

75

78

79

A frequently employed strategy to examine the Sauter-Schwinger mechanism [15–17] for electron-positron pair creation in supercritical electromagnetic fields revolves around the Dirac equation for the electron-positron field operator. In the absence of external fields, the separation between energy eigenstates corresponding to positrons and electrons is straightforward due to the presence of the mass gap,  $2mc^2$ . These distinct subspaces enable a meaningful separation of the full field operator into its positronic and electronic components. However, the situation becomes intricate in the presence of supercritical fields, leading to a partial degeneracy of states within the upper and lower energy continua. This complicates the energy-based separation into solely positronic and electronic states, presenting a key challenge. This challenge is at the crux of the difficulty in disentangling purely positronic properties and defining a clear, time-dependent count of created pairs within the interaction zone.

There have been several works devoted to the challenge of calculating and interpreting time-dependent particle numbers during the interaction. In 2006, Krekora et al. [18] noted interpretational difficulties in associating field-theoretical quantities with properties of particles when projections based on field-free states to identify positronic states were involved. They showed that spatial probability densities inside the interaction zone depend on the choice of the Hilbert subspace on which the field operator is projected. They associated the term "ghost states" with unphysical contributions to spatial

102

103

105

106

107

109

110

111

113

114

115

118

122

123

124

125

126

127

129

130

131

132

134

135

138

139

141

142

147

148

149

151

152

154

155

156

159

160

162

163

164

167

168

170

172

173

175

176

177

180

181

183

184

185

188

189

192

193

194

densities that could not be interpreted as physical probabilities of real particles. In the same year, Gerry et al. [19] showed that for time-dependent subcritical potentials, instantaneous energy eigenstates provide physically meaningful subspaces to define unambiguous time-dependent particle numbers during the interaction. In 2014 [20] and 2016 [21], Dabrowski and Dunne introduced the concept of time-dependent superadiabatic particle numbers for the Schwinger particle production in time-dependent electric fields by truncating (diverging and asymptotic) adiabatic expansions at optimal order. This optimally truncated particle number provided also a clear picture of quantum interference processes, which are responsible for particle production for perturbations with nontrivial temporal substructure. In 2019, Unger et al. [22] provided an alternative formulation to the traditional quantum kinetic Vlasov equation [23], where a projection based on field-free states instead of the instantaneous basis was investigated. It was suggested that the temporal turn-off shape of the external field would determine which approach is physically more meaningful. To further unlock the mysteries of the birth process, recent proposals in 2021 [24] and 2023 [25] employed a machine learning-based approach with the potential to surmount this conceptual hurdle. Here, genetic-programming-based symbolic regression algorithms first learn multiple sequences of partially dressed positronic spatial probability densities as training data and then exploit their features as a function of the dressing strength in order to predict the particles' true distribution in space and momentum. In 2022 Ilderton [26] stressed that in addition to the question about the most suitable basis system a better understanding of the physics implied by the choice for each basis set and what it really counts is crucial. He examined the adiabatic number of pairs introduced in [20,21] and suggested its physical meaning in terms of a very rapid (but not abruptly) turn off of the external field. In 2023, Diez et al. [27] studied the particles' formation length and timescales.

While our work is of fundamental theoretical nature, it is worth noting that this phenomenon of vacuum breakdown in strong external fields is now gaining immense experimental attention, owing to remarkable advancements in high-power laser systems' capabilities [28–32].

The structure of this work is organized as follows: In Sec. II we review our numerical methodology to compute the quasidressed density that describes real positrons and its corrections. In Sec. III we approximate these corrections by the density of positrons that are solely created due to the time dependence of an abruptly changing potential. We provide numerical, perturbative, and phenomenological expressions for these corrections. In Sec. IV we examine the properties of the positron's true density obtained by the proposed subtraction scheme and examine a consistency test to examine its accuracy. We conclude in Sec. V with a brief discussion and an outlook on future research directions.

# II. THE GENERAL FRAMEWORK OF COMPUTATIONAL QUANTUM FIELD THEORY

In this section we briefly review our numerical approach (Sec. II A), and the electronic and positronic subspaces (Sec. II B) required to partition the field operator into its

positronic part (Sec. IIC), which is needed to compute the quasidressed densities (Sec. IID). We also introduce the concept of abruptons, which is essential to correctly interpret the physical meaning of spatial densities inside the interaction zone. The review parts of Secs. (IIA) to (IIC) can be skipped by readers who are already familiar with the basic idea of computational quantum field theory (CQFT).

### A. The total electron-positron field operator

In contrast to many other powerful approaches to study strong-field quantum electrodynamics (QED) effects, where dressed propagators, S matrices, Feynman graphs, worldline instantons, Wigner functions, *n*-point correlation functions, scattering cross sections, spectra, and vacuum expectation values serve as the central quantities in CQFT, the fundamental quantity of interest is the fully correlated electron-positron field operator  $\Psi(z,t)$ . Its space-time evolution can be obtained from multiple wave-function solutions to the Dirac equation. If the spatial dimension is reduced to 1, it is possible to use a finite space-time grid to evaluate this operator exactly without any further approximation. For example, by introducing fermionic creation and annihilation operators associated with a certain Hilbert state basis, the quantum field theoretical operator  $\Psi(z,t)$  as a function of time t and position z can be expanded [33,34] as the summations

$$\begin{split} \Psi(z,t) &= \Sigma_p b_p(t) \phi_p(u;z) + \Sigma_p d_p^{\dagger}(t) \phi_p(d;z) \quad (2.1a) \\ &= \Sigma_p b_p \phi_p(u;z,t) + \Sigma_p d_p^{\dagger} \phi_p(d;z,t). \quad (2.1b) \end{split}$$

Traditionally,  $\phi_p(u;z,t)$  and  $\phi_p(d;z,t)$  are chosen as the complete set of wave functions evolved in time under the general Dirac Hamiltonian (in one spatial dimension):

$$H(V_0) = c \sigma_1[p - e A(z, t)/c] + \sigma_3 mc^2 + e V(z, t)$$
 (2.2)

where eV is the interaction energy and e and m are the positron's charge and mass. The solution technique is general enough to be applied to any vector potential A(z,t) and scalar potential V(z,t). However, for better clarity we consider in this work the case where A(z,t)=0 and where the potential  $V(z,t)=V_0(mc^2/e)$   $V_s(z)$  f(t). Here,  $f(t)\equiv \sin^2[\pi t/(2T_{on})]$  for  $t< T_{on}$  and  $f(t)\equiv 1$  for  $T_{on}< t$  governs the type of temporal turn on and the (scaled) electrostatic potential  $V_s(z)$  changes from  $V_s(z\to-\infty)\equiv 1$  and to  $V_s(z\to\infty)\equiv 0$ . For the dynamics of interest, we will choose the (scaled) unitless amplitude  $V_0=5$ , which makes the system supercritical. The corresponding spatially localized supercritical electric field follows as E(z)=-dV(z)/dz.

The initial states  $\phi_p(u;z,t=0)$  and  $\phi_p(d;z,t=0)$  are the energy eigenstates of the force-free Dirac Hamiltonian, given by  $H_0 \equiv c \, \sigma_1 \, p + \sigma_3 \, mc^2$ , where p labels again their momentum. They fulfill  $H_0\phi_p(u;z) = e_p\phi_p(u;z)$  and  $H_0\phi_p(d;z) = -e_p\phi_p(d;z)$  with  $e_p \equiv [m^2c^4 + c^2p^2]^{1/2}$ . It is important to note that the operator solution  $\Psi(z,t)$  does not depend on which particular set of basis states has been chosen for the mode expansion in Eqs. (2.1).

In general, the characteristic spatial and temporal scales for the electron-positron dynamics are naturally provided by the fermions' Compton wavelength  $\lambda \equiv \hbar/(\text{mc}) = 3.8 \times 10^{-13} \text{ m}$  and the time  $T \equiv \hbar/(\text{mc}^2) = 1.3 \times 10^{-21} \text{ s}$ . Below, we use  $\lambda$ 

and T as the basic units for the presentation of our numerical data.

## B. Positronic and electronic subspaces of the partially dressed Dirac Hamiltonian

If the potential is chosen supercritical (i.e.,  $V_0 > 2$ ), then the usual mass gap between the energy eigenstates of positive and negative energy disappears and some of the states become energy degenerate. This means that a unique and unambiguous (energy-based) distinction between electronic and positronic subspaces is no longer possible. This separation is only possible if the unitless amplitude (which we denote from now on with  $\alpha$ ) of the potential  $\alpha$  (mc²/e)V<sub>s</sub>(z) is chosen less than 2, i.e., for a Hamiltonian:

$$H(\alpha) \equiv c \sigma_1 p + \sigma_3 m c^2 + \alpha mc^2 V_s(z). \tag{2.3}$$

Obviously, for  $\alpha \to V_0$ , this Hamiltonian  $H(\alpha)$  becomes identical to the fully dressed Hamiltonian H. If  $\alpha < 2$ , the potential is subcritical and the energy of the eigenstates of  $H(\alpha)$  can be used as a yardstick to separate unambiguously between purely positronic and electronic states. These corresponding (partially dressed) eigenstates are defined as  $H(\alpha) \phi_P(u,z;\alpha) = E_{u,P}(\alpha) \phi_P(u,z;\alpha)$  and  $H(\alpha) \phi_P(d,z;\alpha) = E_{d,P}(\alpha)\phi_P(d,z;\alpha)$ , with  $E_{u,P}(\alpha)$  and  $E_{d,P}(\alpha) < mc^2$ .

## C. Separation of the electron-positron field operator into its positronic portion

Ideally, in order to compute an unambiguous spatial number density for the created positrons  $\rho(e^+,z,t)$ , we have to partition first the electron-positron field operator  $\Psi(z,t)$  into its positronic contribution. To calculate a "true" field operator for the positrons only, we would need to project the full field operator at any time onto the subspace of positronic states for  $\alpha = 5$ . However, due to the unavoidable energy degeneracy mentioned above, for  $\alpha > 2$  the required states  $\phi_P(u,z;\alpha)$ for the corresponding projector cannot be identified based on energetic considerations. Therefore, we can only define the positronic (electronic) portions of the field operator for the dressing parameters  $\alpha$  that are less than 2. Here, using a projection of the (fully dressed) electron-positron field operator  $\Psi(z,t)$  onto the Hilbert space of partly dressed energy eigenstates  $|P_{\alpha}\rangle$  of positive energy, one can introduce a positronic (and electronic) part of the operator,

$$\begin{split} &\Psi(e^+,z,t;\,\alpha,\,V_0)\\ &\equiv \Sigma_{P\alpha}|P_\alpha\rangle\langle P_\alpha|\Psi(z,t)\\ &= \Sigma_{P\alpha}\phi_P(u,z;\alpha)\int dz'\phi_P(u,z',\alpha)^\dagger\Psi(z',t), \qquad (2.4a)\\ &\Psi(e^-,z,t;\alpha,\,V_0)\\ &\equiv \Sigma_{P\alpha}C\phi_P(d,z;\alpha)\int dz'\phi_P(d,z',\alpha)^\dagger\Psi(z',t). \quad (2.4b) \end{split}$$

Here, C denotes the antiunitary charge-conjugation operator. As each value of  $\alpha$  characterizes its own set of energies (labeled by  $P_{\alpha}$ ), the projected operator  $\Psi(e^+,z,t;\alpha,V_0)$  does depend on  $\alpha$ . These positronic (partly dressed) states  $|P_{\alpha}\rangle$  can be calculated as the energy eigenstates for the fully coupled

Dirac Hamiltonian, but the amplitude (denoted by  $\alpha$ ) has to be subcritical, instead of the supercritical value  $V_0=5$  used to compute the dynamics for  $\Psi(z,t)$ . We can define the positronic quasinumber density by the vacuum expectation value:

$$\rho(e^+, z, t; \alpha, V_0) \equiv \langle \Psi^{\dagger}(e^+, z, t; \alpha, V_0) \Psi(e^+, z, t; \alpha, V_0) \rangle$$
(2.5)

We should mention that two prior works [24,25] referred to in the Introduction have explored some sophisticated machine-learning techniques to use sequences of quasidensities for  $\rho(e^+, z, t; \alpha, V_0)$  for several dressing strengths  $\alpha$  < 2 to predict  $\rho(e^+, z, t; \alpha = V_0)$  for the supercritical value  $\alpha = V_0$ .

Using Eqs. (2.1), (2.4a), and (2.5), the time dependence of the total number of positrons according to  $N(\alpha, V_0, t) \equiv \int dz$   $\rho(e^+, z, t; \alpha, V_0)$ , can be evaluated to

$$N(\alpha, V_0, t) = \sum_n \sum_{P\alpha} |\langle P_\alpha | n(t) \rangle|^2, \qquad (2.6)$$

where  $|n(t)\rangle$  denotes the time-evolved energy eigenstate of  $H_0$ . This expression also nicely formalizes the traditional Dirac picture for pair creation, where the initial bare vacuum state is represented by all negative energy eigenstates  $|n\rangle$ . If under the time evolution  $|n\rangle$  can excite any eigenstate of the subspace of the positive-energy eigenstates of  $H(\alpha)$ , we interpret this transition with the creation of a positron into the positive-energy state  $|P_{\alpha}\rangle$ . As the total number of created positrons is equal to the number of electrons, we can omit the label  $e^+$  in  $N(\alpha, V_0, t)$ . Similarly, the resulting quasidressed spatial density of the positrons amounts to

$$\rho(e^+, z, t; \alpha, V_0) = \sum_{n} |\sum_{P\alpha} \langle P_{\alpha} | n(t) \rangle \phi_P(u, z, \alpha)|^2 \quad (2.7)$$

## D. The quasidressed density $\rho(e^+, z, t; \alpha, V_0)$ describes real positrons and corrections

During the time evolution, the computed "quantity"  $\rho(e^+, z, t; \alpha, V_0)$  defined in Eqs. (2.5) and (2.7) describes both real physical positrons and (unfortunately) also mathematical contributions. The part that corresponds to the real spatial distribution of positrons, denoted by  $\rho_{phys}(e^+, z, t, V_0)$ , cannot depend on the dressing parameter  $\alpha$ . Far outside the paircreation zone, where the electric field is zero, we should consistently have  $\rho(e^+, z, t; \alpha, V_0) = \rho_{phys}(e^+, z, t, V_0)$ . This is fully consistent with the fact that the spatial form of the energy eigenstates outside the interaction zone (where  $V_s = 0$  or  $V_s = 1$ ) is independent of  $\alpha$ . The key problem is, of course, to compute the true positronic particle density  $\rho_{phys}(e^+, z, t, V_0)$  inside the interaction zone.

In order to obtain the true observable density of physical positrons at a given time t, it is necessary to project the evolved field operator  $\Psi(z,t)$  onto the corresponding submanifold of instantaneous energy eigenstates of the true Dirac Hamiltonian associated with positrons at that moment in time. For instance, if the potential is zero at a specific time t (or, equivalently, turned off abruptly to zero at time t), then the projection should be performed on the completely force-free  $(\alpha=0)$  energy eigenstates to obtain the true particle density. This means that the (commonly studied) time-dependent density  $\rho(e^+,z,t;\alpha=0,V_0)$  (based on the popular projection onto force-free states) corresponds only to the true density at time t if the potential's amplitude  $V_0$  was suddenly

296

297

299

300

303

304

305

307

308

311

312

313

315

316

319

320

321

323

324

328

329

330

331

332

333

334

336

337

338

340

341

342

346

347

348

350

351

352

355

356

359

360

363

364

365

367

368

371

372

373

375

378

379

381

382

386

387

388

390

391

394

395

398

399

400

402

turned off to  $V_0 = 0$  at that time t. However, it is crucial to acknowledge that due to the (unavoidable) time dependence of (even an abrupt) turn off, shape of the potential additional pair annihilation and creation processes are triggered. The possibility of the resulting change in the particle number is already fully contained in  $\rho(e^+, z, t; \alpha = 0, V_0)$  at any time t. In essence, this means that  $\rho(e^+, z, t; \alpha = 0, V_0)$  describes a combination of the real physical particles present at that interaction time t together with those particles that would be created or annihilated solely as a result of a sudden turn-off process of the field to zero. A comprehensive understanding of these latter particles is crucial for the core of this study. Consequently, we term these particles, which arise as a consequence of the sudden turn-off process, as "abruptons" and denote their associated spatial density with  $\rho_{abr}$ . It is essential to emphasize that the concept of abruptons emerges from a particular projection approach (i.e., when  $\alpha$  is not equal to  $V_0$ ), and their existence is purely mathematical at this stage. Only after an infinitesimal time period following the abrupt change in the potential strength do they manifest as physical particles with observable properties.

In a more general scenario, when the (scaled) potential strength is equal to  $\alpha$  (or is suddenly changed to  $\alpha$ ), a different projection process is required for meaningful densities. We must now project onto the positronic energy eigenstates associated with the potential of strength  $\alpha$ . As a result, the quasidensity  $\rho(e^+, z, t; \alpha, V_0)$  for  $\alpha \neq 0$  gains a clear and unambiguous interpretation. It represents the true physical density if the amplitude of the potential V<sub>0</sub> becomes time dependent and is abruptly changed from any value  $V_0$  to  $\alpha$ at time t. In that sense,  $\rho(e^+, z, t; \alpha, V_0)$  carries too much information. It encompasses both real particles and those additional particles that are created under a possible abrupt change of the potential from  $V_0$  to the value  $\alpha$ . This further emphasizes the importance of considering both types of particles in our analysis when examining the physical density at a given time t under such conditions.

# III. THE MAIN STRATEGY: ESTIMATE THE SPATIAL DISTRIBUTION $\rho_{corr}(e^+, z; \alpha, V_0)$

In this work, we focus on the asymptotic long-time situation, where the supercritical electric field region acts as a constant source of created particles. Here, we try to examine the steady-state distributions of the positrons inside the interaction region. The computationally obtained steady state density  $\rho_{\text{steady}}(e^+, z; \alpha, V_0)$  can be decomposed into a density  $\rho_{\text{phys}}$  that describes the true physical positrons, and a correction term  $\rho_{\text{corr}}$  that we will try to associate below with abruptons:

$$\rho_{\text{steady}}(e^{+}, z; \alpha, V_{0})$$

$$= \rho_{\text{phys}}(e^{+}, z; V_{0}) + \rho_{\text{corr}}(e^{+}, z; \alpha, V_{0})$$
 (3.1)

We note that this general expression is exact and not just an assumption. Depending on the specific type of particle population inside the interaction, an abrupt change of the external field from  $V_0$  to  $\alpha$  can create but possibly also annihilate positrons [19]. This means that the mathematical (correction)

term  $\rho_{corr}(e^+, z; \alpha, V_0)$  does not even have to be strictly positive in all situations.

In addition to an unambiguous interpretation of  $\rho_{abr}(e^+, z; \alpha, V_0)$  (accomplished in Sec. II D), the second central goal of this work is to obtain a quantitative understanding of this particular correction term. While  $\rho_{phys}(e^+, z; V_0)$  obviously cannot depend on  $\alpha$ , the correction term  $\rho_{corr}(e^+, z; \alpha, V_0)$  does depend on  $\alpha$ . In other words, if we were able to construct the functional properties of  $\rho_{corr}(e^+, z; \alpha, V_0)$ , we could simply subtract it from the computationally available solution  $\rho_{steady}(e^+, z; \alpha, V_0)$ . In this way, we would be able to use these computational data to determine the ultimate goal, i.e.,  $\rho_{phys}(e^+, z; V_0)$ .

To have concrete numerical examples in this work, we have examined two electric field shapes, both of which of total extension d and vanish for |z| > d/2. The first one is constant with amplitude  $E_0 \equiv V_0 \text{mc}^2/(\text{ed})$  for -d/2 < z < d/2 and  $E_0 = 0$  for |z| > d/2. Here, the corresponding (scaled) potential decreases linearly, i.e.,  $V_s(z) = 1$  for z < -d/2,  $V_s(z) = 1 - (z/d + 1/2)$  for -d/2 < z < d/2, and  $V_s(z) = 0$  for d/2 < z. In order to study an electric field configuration with a more interesting spatial substructure, we have also chosen a three-peaked electric field, given by  $E(z) = E_0 \cos^4[3\pi z/d]$  for -d/2 < z < d/2 and E(z) = 0 for |z| > d. In this case, the corresponding (scaled) potential is  $V_s(z) = 1$  for z < -d/2,  $V_s(z) = 1 - [18\pi(1 + 2z/d) + 8\sin(6\pi z/d) + \sin(12\pi z/d)]/(6\pi)$  for -d/2 < z < d/2 and  $V_s(z) = 0$  for d/2 < z.

### A. Approximations for the spatial distribution $\rho_{corr}(e^+, z; \alpha, V_0)$

The best way to visualize abruptons is to consider the dynamics associated with a subcritical potential, which cannot generate any permanent flux of created particles; therefore, any particles that occur must have been generated exclusively by temporally triggered transitions during those moments in time when the potential was turned on or turned off. This situation is precisely what was examined in 2006 by Gerry et al. [19]. Here, the number of created particles during an abrupt turn on was compared to the number of created particles during the turn off. Here, a remarkable symmetry was observed. It was shown that if the timespan between the turn on and turn off was sufficiently long such that those particles that were created during the turn on had sufficient time to escape from the interaction region, then the number of created particles during the turn-off interval was identical to the number of created particles during the turn on. In fact, even the spatial densities of the created positrons during the abrupt turn on and turn off were identical. This is an important observation with regard to this present work.

The main theme of our present work is to explore and test the implications of the following hypothesis: We will approximate the density  $\rho_{corr}(e^+, z; \alpha, V_0)$  required for the supercritical situation in Eq. (3.1) with the density of created particles during the sudden turn off from potential  $V_0$  to  $\alpha$ , which we have denoted above with  $\rho_{abr}(e^+, z; \alpha, V_0)$ . In the same vein, we will also examine the dependence of number of created particles, defined as  $N_{abr}(\alpha, V_0) \equiv \int dz \, \rho_{abr}(e^+, z; \alpha, V_0)$  as a function of  $\alpha$  and  $V_0$ .

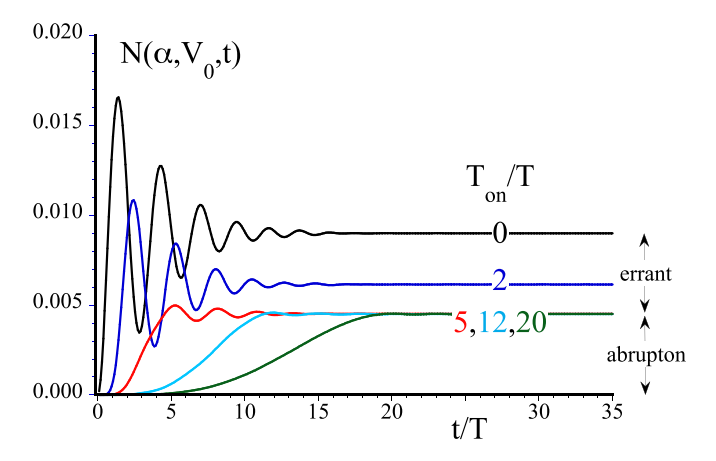


FIG. 1. The temporal growth of the number of positrons  $N(\alpha=0,V_0=2,t)$  [according to the definition in Eq. (2.6)] for different dynamics, characterized by five turn-on durations  $T_{\rm on}$  to ramp up the linear potential V(z) to the subcritical value  $V_0=2$  via the turn-on shape  $f(t)=\sin^2(\pi t/(2T_{\rm on}))$ . The numerical parameters are the box size  $L=219.3~\lambda~(=1.6~{\rm a.u.}),~N_z=2048$  spatial grid points,  $N_t=300$  temporal grid points, and the spatial extension of the constant electric field is  $d=10~\lambda$ .

# B. Scaling features of the spatial distribution $\rho_{abr}(e^+,z;\alpha,V_0)$ and of $N_{abr}(\alpha,V_0)$

Before we can develop a theoretical handle on the purely projection-based contributions to  $\rho$  and to N, we have to eliminate the true physical positrons that are created during time dependence of the subcritical potential during its turn on. As a first step, in Fig. 1 we have computed the time-dependent number of positrons defined here as  $N(\alpha,V_0,t) \equiv \int dz \, \rho(e^+,z,t;\alpha=0,V_0)$ , based on the (force-free) basis for  $\alpha=0$  for five temporal turn-on durations  $T_{\rm on}$ , ranging from an abrupt turn on  $(T_{\rm on}=0)$  to a very slow adiabatic turn on  $(T_{\rm on}=20\,{\rm T})$ .

We start our discussion of Fig. 1 with the data for sufficiently large turn-on durations ( $T_{\rm on} > 5\,\rm T$ ). Here, the number of created particles (according to the density obtained by the projection based on  $\alpha=0$ ) approaches the value N=0.0045, which is independent of the duration of the turn on. Furthermore, here the density  $\rho(e^+,z,t;\alpha=0,V_0)$  becomes independent of time and vanishes outside the interaction zone. This mathematical density describes exactly the true physical positrons that would be created if the strength of the subcritical potential  $V_0$  was turned off abruptly to  $V_0=0$ . This means that if we repeat our simulations but calculate the long-time density  $\rho(e^+,z,t;\alpha=0,V_0)$  for  $\alpha=0$ , we can obtain the desired density  $\rho_{abr}(e^+,z;V_0,\alpha=0)$ . A similar technique allows us to determine  $\rho_{abr}(e^+,z;\alpha,V_0)$  for  $\alpha\neq 0$  but less than 2

For completeness, a short comment about the dynamics for shorter turn-ons ( $T_{\rm on} < 2\,\rm T$ ) is in order. Here, we should mention that the additional number of positrons associated with the case of a faster turn on in Fig. 1 corresponds to those real particles that were created during the turn on. These real positrons were named "errants" in Ref. [35], as they escape the interaction symmetrically, i.e., independent of the direction of the electric force. Evidently, these errants are also

created during a sudden turn off. However, for the case of an adiabatic turn on or turn off they are not generated, as the frequency spectrum of the turn-on or off shape does not contain sufficiently large frequencies to trigger any upwards transition into the positive-energy continuum.

Therefore, we have established two fully equivalent computational techniques to generate  $\rho_{abr}(e^+,\,z;\,V_0\to\alpha)$  and also  $N_{abr}(\alpha,V_0)\equiv\int dz\,\rho_{abr}(e^+,\,z;\,\alpha,\,V_0).$  We can either use an abruptly turned-on external field, wait until all errants have escaped the interaction zone, and then use the remaining probability density inside this zone as  $\rho_{abr}(e^+,\,z;\,\alpha,\,V_0)$  or  $N_{abr}(V_0,\,\alpha)$ , or to avoid any errants entirely we can adiabatically ramp up the field to  $V_0.$ 

In Fig. 2 we have graphed the resulting  $N_{abr}(\alpha,V_0)$  obtained as the final "population" inside the interaction zone for a subcritical (and abruptly turned-on) potential of strength  $V_0=2$  for 11 dressing parameters  $\alpha.$ 

As expected, after a time of about 25 T,  $N_{abr}(\alpha, V_0)$  approaches a constant value. It is interesting that the usual initial violent oscillations for very short times are completely absent for  $\alpha = V_0 = 2$ . Fully consistent with our expectation, we also observe here that for  $\alpha = V_0 = 2$  the final value for  $N_{abr}(\alpha, V_0)$  vanishes as  $V_0$  was subcritical.

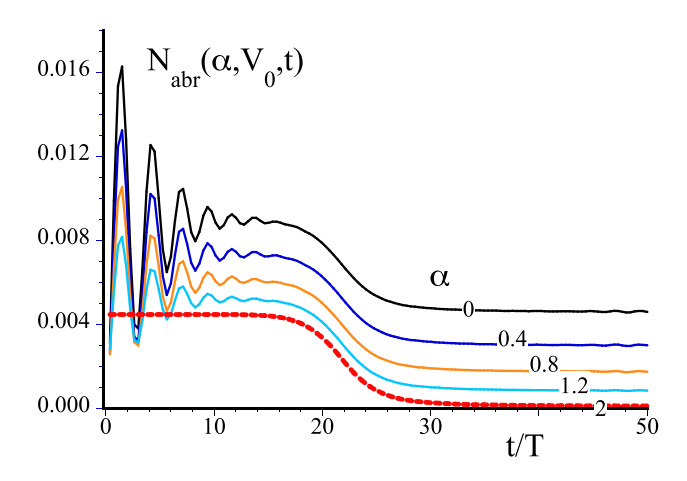
In order to explore how  $N_{abr}(\alpha,V_0)$  scales with  $V_0$  and  $\alpha$ , we have graphed it in Fig. 2(b) as a function of the dressing parameter  $\alpha$  for five different values of  $V_0$ . The perfectly parabolic data suggest a remarkable symmetry of  $N_{abr}(\alpha,V_0)$ . In the entire region for  $0 < V_0 < 2$  and  $0 < \alpha < 2$ , we find that  $N_{abr}(z; V_0 \to \alpha)$  does not depend in a complicated way on  $V_0$  and  $\alpha$  independently, but it is solely a function of the difference  $(V_0 - \alpha)^2$  and graphically nearly indistinguishable from the function

$$N_{abr}(\alpha, V_0) = 0.0011 (V_0 - \alpha)^2$$
. (3.2)

Furthermore, more generally, it turns out that this expression is fully valid for  $-2 < V_0 < 2$  and  $-2 < \alpha < 2$ , i.e., it does not even matter in which direction the electric field points. This extended scaling property is extremely helpful for our analysis of the supercritical case ( $V_0 = 5$  and  $\alpha < 2$ ), where  $|V_0 - \alpha| = 3$ . Here, the density  $\rho_{abr}(e^+, z; \alpha, V_0)$  [to be subtracted from  $\rho_{steady}(e^+, z; \alpha, V_0)$ ] could be calculated from the easier subcritical case where  $V_0 = 1$  and  $\alpha = -2$  or the case  $V_0 = 2$  and  $\alpha = -1$ .

## C. Perturbative confirmation of the scaling properties of $\rho_{abr}(e^+, z; \alpha, V_0)$ and of $N_{abr}(\alpha, V_0)$

The observation that the density  $\rho_{abr}(e^+, z; \alpha, V_0)$  as well as the number  $N_{abr}(\alpha, V_0)$  associated with  $V_0$  can be generated by turning the potential on very slowly, i.e. adiabatically, suggests a possible approximation scheme to provide some analytical support to confirm its observed scaling properties with regard to difference  $(V_0-\alpha)^2$ . Under the condition of an adiabatic change of the potential from strength  $\alpha$  to  $V_0$ , any initial energy eigenstate of  $H(\alpha)$  evolves in time in such a way that it remains an instantaneous eigenstate of the corresponding Hamiltonian. In other words, the true final state  $|P_{\alpha}(t)\rangle$  associated with the initial state  $|P_{\alpha}\rangle$  can be approximated by  $|P_{V_0}\rangle$ . As a second assumption, we use the usual Raleigh-Schrödinger perturbation theory, to express



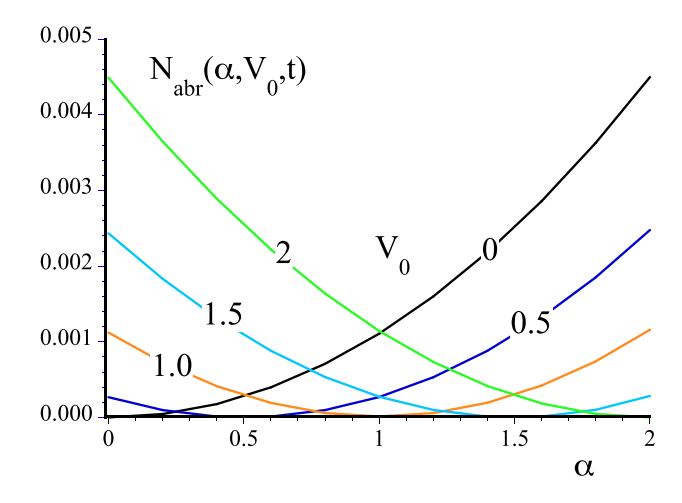


FIG. 2. (a) The time evolution of the number of positrons  $N_{abr}(\alpha,V_0,t)$  [according to the definition in Eq. (2.6)] for 11 values of the dressing parameter  $\alpha$  used in the projection operator and  $V_0=2$ . The linear potential V(z) of subcritical strength  $V_0=2$  and extension  $V_0=1$ 0 was turned on abruptly. (b) The final number of positrons  $V_0=1$ 1 time  $V_0=1$ 1 time  $V_0=1$ 1 (=0.006 a.u.) as a function of the dressing strength  $V_0=1$ 1 five different subcritical dynamics with strength  $V_0=1$ 1 time  $V_0=1$ 1.

the eigenstate  $|P_{V_0}\rangle$  for  $V_0$  in terms of the set of "unperturbed" states  $|P_{\alpha}\rangle$  and  $|N_{\alpha}\rangle$  associated with  $H(\alpha)$ . We can

write  $H(V_0) = H(\alpha) + (V_0 - \alpha) \text{ mc}^2 V_s(z)$ , i.e., and therefore we consider  $(V_0 - \alpha) \text{ mc}^2 V_s(z)$  as the perturbation. We obtain

$$|P_{V_0}\rangle = |P_{\alpha}\rangle + (V_0 - \alpha) \operatorname{mc}^2 \Sigma_{P\alpha'} \langle P_{\alpha'} | V_s(z) | P_{\alpha'} \rangle / (E_{P\alpha} - E_{P\alpha'}) | P_{\alpha'} \rangle + (V_0 - \alpha) \operatorname{mc}^2 \Sigma_{N\alpha'} \langle N_{\alpha'} | V_s(z) | P_{\alpha} \rangle / (E_{P\alpha} - E_{N\alpha'}) | N_{\alpha'} \rangle$$
(3.3)

If we insert this first-order solution in  $O(V_0-\alpha)$  for  $|P_{V_0}\rangle$  into the expression of Eq. (2.6), we obtain

499

501

502

503

505

506

507

$$\begin{split} N_{abr}(\alpha,V_0) \\ &= (V_0 \! - \! \alpha)^2 m^2 c^4 \Sigma_{N\alpha} \Sigma_{P\alpha} |\langle N_\alpha | V_s(z) | P_\alpha \rangle / (E_{P\alpha} \! - \! E_{N\alpha})|^2 \end{split} \label{eq:Nabr}$$
 (3.4)

In order to check the numerically suggested simple scaling  $N_{abr}(\alpha,V_0)\sim (V_0-\alpha)^2$ , we have to confirm that the expression for the double summation  $\Sigma\Sigma\equiv\Sigma_{N\alpha}\,\Sigma_{P\alpha}|\langle N_\alpha|V_s(z)|P_\alpha\rangle/(E_{P\alpha}-E_{N\alpha})|^2$  does not depend very sensitively on  $\alpha$  or  $V_0$ . The independence on  $V_0$  is trivial; however, to examine the dependence on  $\alpha$  requires the numerical evaluation of the double sum  $\Sigma\Sigma$ . In Table I we have summarized the numerical value of this double sum

TABLE I. The double sum  $\Sigma\Sigma$  defined in Eq. (3.4) for linear potentials  $V_s(z)$  with three different extensions d.

α	$\Sigma  \Sigma$ for $d=10  \lambda$	$\Sigma\Sigma$ for $d=15~\lambda$	$\Sigma \Sigma$ for $d = 20 \lambda$
-2.0	0.001204	0.0007728	0.0005781
-1.5	0.001143	0.0007629	0.0005742
-1.0	0.001121	0.0007563	0.0005712
-0.5	0.001108	0.0007524	0.0005696
0.0	0.001104	0.0007512	0.0005691
0.5	0.001108	0.0007524	0.0005696
1.0	0.001121	0.0007563	0.0005712
1.5	0.001143	0.0007629	0.0005741
2.0	0.001204	0.0007728	0.0005781

of the linear potential given by  $V_s(z)$  with three different extensions d.

508

511

512

513

514

515

516

517

518

520

521

524

525

528

529

530

532

The data in the table confirm that the double sum  $\Sigma\Sigma$  depends only very weakly on  $\alpha$ . In other words, the first-order perturbation theory (together with the assumption of adiabaticity) confirms the overall observed scaling behavior  $N_{abr}(\alpha, V_0) \sim (V_0 - \alpha)^2$ .

Very similarly, the same methodology can also be applied to approximate perturbatively the positronic density, which we obtain as

$$\rho_{abr}(e^{+}, z; \alpha, V_{0})$$

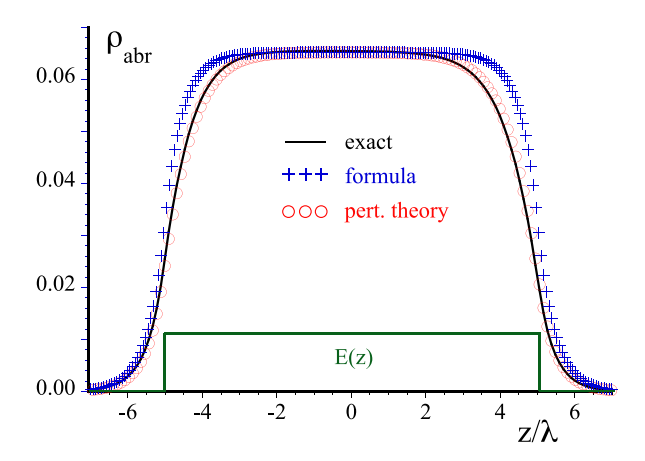
$$= (V_{0}-\alpha)^{2} m^{2} c^{4} \Sigma_{N\alpha}$$

$$|\Sigma_{P\alpha} \langle P_{\alpha} | V_{s}(z) | N_{\alpha} \rangle / (E_{N\alpha} - E_{P\alpha}) \phi_{P}(u, z, \alpha)|^{2}$$
 (3.5)

In order to examine if the density is solely a function of  $(V_0-\alpha)^2$ , we have computed numerically the second factor  $\Sigma\Sigma(z) \equiv \Sigma_{N\alpha} |\Sigma_{P\alpha} \langle P_\alpha | V_s(z) | N_\alpha \rangle / (E_{N\alpha} - E_{P\alpha}) \phi_P(u,z,\alpha)|^2$ . In Fig. 3 we display the scale-independent densities for  $\alpha=0$  for the constant as well as the three-peaked electric field.

Here, the exact densities for  $(\alpha = 0, V_0 = 2)$  and  $(\alpha = 2, V_0 = 0)$  are graphically indistinguishable from each other. Also, the agreement with the perturbative predictions according to Eq. (3.5) is excellent.

We should conclude this section by proposing an approximate quasiphenomenological expression to relate the shape of the electric field  $E_s(z)$  (=  $-dV_s(z)/dz$ ) directly to  $\rho(e^+,z,t;\alpha,V_0)$ . This convolution integral-type expression assumes some kind of linearity and that a very sharp delta-functionlike electric field leads at turn off to a spatially exponentially decaying



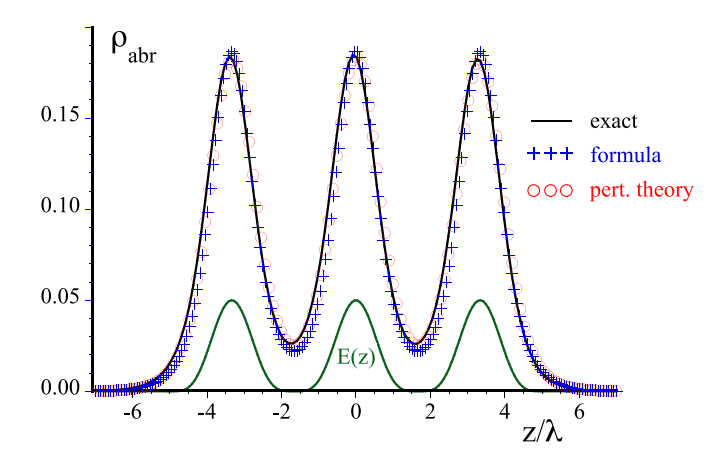


FIG. 3. Comparison of the (scaled) abrupton density  $\rho_{abr}(e^+, z, \alpha, V_0)$  obtained exactly numerically, with the predictions of perturbation theory [Eq. (3.5)] and of the phenomenological convolution integral  $\sim \int dx \, E^2(x) \, \exp[-2.2 \, |z-x|/\lambda]$  for  $d=10\lambda$ ,  $V_0=2$ , and  $\alpha=0$ . For comparison, we also sketch the spatial shape of the electric field. All other parameters as in Fig. 1, (a) for the constant electric field, (b) for the three-peaked electric field.

density on a scale of  $\lambda$ . This point-spread function integral [25,35–38] reads, for  $d = 10 \lambda$  and  $E_c^2(z) = \theta(d/2-|z|)$ ,

$$\begin{split} \rho_{abr}(e^+, \ z, \alpha, \ V_0) \\ &= (V_0 - \alpha)^2 0.01632 (e^2 m^{-2} c^{-4}) \\ &\times \int dx \ (1.1/\lambda) \exp[-2.2|z - x|/\lambda] E_s^2(x) \quad (3.6) \end{split}$$

In Fig. 3 we have superimposed this prediction by the crosses and find a qualitative agreement with the exact data for the constant as well as the three-peaked electric field. While this expression approximates the computed density, it also raises an interesting conceptual question about locality and the nontrivial choice for the relativistic position operator in quantum field theory [39–44]. We note that the finite width of the integration kernel  $\sim \lambda$  predicts the density  $\rho_{abr}(e^+, z, \alpha, V_0)$  to be nonzero, even in those spatial regions (z > |d/2|), where the electric field vanishes.

### IV. THE PHYSICAL POSITRON SPATIAL DENSITY

As we have now obtained a good understanding of the scaling properties of the density  $\rho_{corr}(e^+, z; \alpha, V_0)$  and even quasianalytical approximations, we can now subtract it from the computed density  $\rho_{steady}(e^+, z; \alpha, V_0)$  for a supercritical potential with  $V_0 = 5$ . In Sec. IVB we will provide some consistency tests based on the total charge density that give us some estimate of the accuracy of this subtraction scheme.

# A. The positron spatial density in the steady state for several supercritical fields

We can now analyze the features of the difference  $\rho_{steady}(e^+,z;\alpha,V_0)-\rho_{abr}(e^+,z;\alpha,V_0)$  as a potential candidate for the desired density  $\rho_{phys}(e^+,z,V_0)$ .

In Fig. 4(a) we present the original density  $\rho_{\text{steady}}(e^+, z; \alpha, V_0)$  for  $V_0 = 5$  for five different values of the dressing parameters,  $\alpha = 0$ , 0.5, 1.0, 1.5, and 2.0. The rather strong dependence of  $\rho_{\text{steady}}$  on  $\alpha$  inside the interaction region of the constant electric field is obvious. As expected, outside this region,  $\rho_{\text{steady}}(e^+, z; \alpha, V_0)$  is constant and independent of  $\alpha$ .

As the electric field was positive (i.e., pointing to the right) the positrons are ejected exclusively to  $z \to \infty$ . We remark that the constant value of  $\rho_{\text{steady}}(e^+, z; \alpha, V_0)$  for z > d/2 can also be obtained from time-independent methods, such as Hund's rule [37,38].

In order to examine the quality of our proposed subtraction scheme, we have also graphed the difference  $\rho_{steady}(e^+,z;\alpha,V_0)-\rho_{abr}(e^+,z;\alpha,V_0)$  for the three values of  $\alpha=1.0,\ 1.5,\ and\ 2.0.$  These were obtained from subcritical simulations with  $(\alpha=-2,V_0=2)$  for  $\rho_{steady}(e^+,z;\alpha=1,V_0),\$ with  $(\alpha=-1.5,V_0=2)$  for  $\rho_{steady}(e^+,z;\alpha=1.5,V_0)$  and finally with  $(\alpha=-1,V_0=2)$  for  $\rho_{steady}(e^+,z;\alpha=2,V_0),\$ respectively. The three "corrected" densities suggest that after the subtraction with  $\rho_{abr}$ , the undesirable dependence on  $\alpha$  is significantly reduced. This gives us some evidence that even in the supercritical case a major contribution to  $\rho_{steady}(e^+,z;\alpha,V_0)$  is indeed provided by  $\rho_{abr}(e^+,z;\alpha,V_0).$ 

To convince us of the quality of the reduction of the  $\alpha$  independence also for more general spatially inhomogeneous electric fields, we have repeated in Fig. 4(b) the corresponding data for the three-peaked electric field. Quite interestingly, we see a clear shift of the three peak locations in the direction of the electric field. While the near independence of  $\alpha$  in  $\rho_{\text{steady}} - \rho_{\text{abr}}$  is encouraging, there is unfortunately still a very small  $\alpha$  dependence even after the subtraction. Therefore, we can associate  $\rho_{\text{steady}}(e^+, z; \alpha, V_0) - \rho_{\text{abr}}(e^+, z; \alpha, V_0)$  with  $\rho_{\text{phys}}(e^+, z; V_0)$  only approximately.

In order to examine the remaining  $\alpha$  dependence for several supercritical values of  $V_0$ , we illuminate it from the perspective of the number of positrons inside the interaction zone  $N_{inside}(e^+, \alpha; V_0)$  computed as  $N_{inside}(e^+, \alpha; V_0) \equiv \int dz \, \rho_{steady}(e^+, z; V_0, \alpha)$ , where the spatial integration extends only from z = -d/2 to z = d/2 covering only the region where the electric field is nonzero.

In Fig. 5 we display the numerically obtained (uncorrected)  $N_{inside}(e^+, \alpha; V_0)$  as a function of  $\alpha$  for six supercritical potential strengths. Consistent with our expectation, we find that  $N_{inside}(e^+, \alpha; V_0)$  decreases with increasing  $\alpha$ , as we have here  $\alpha < V_0$  and the magnitudes of the abruptons shrink.

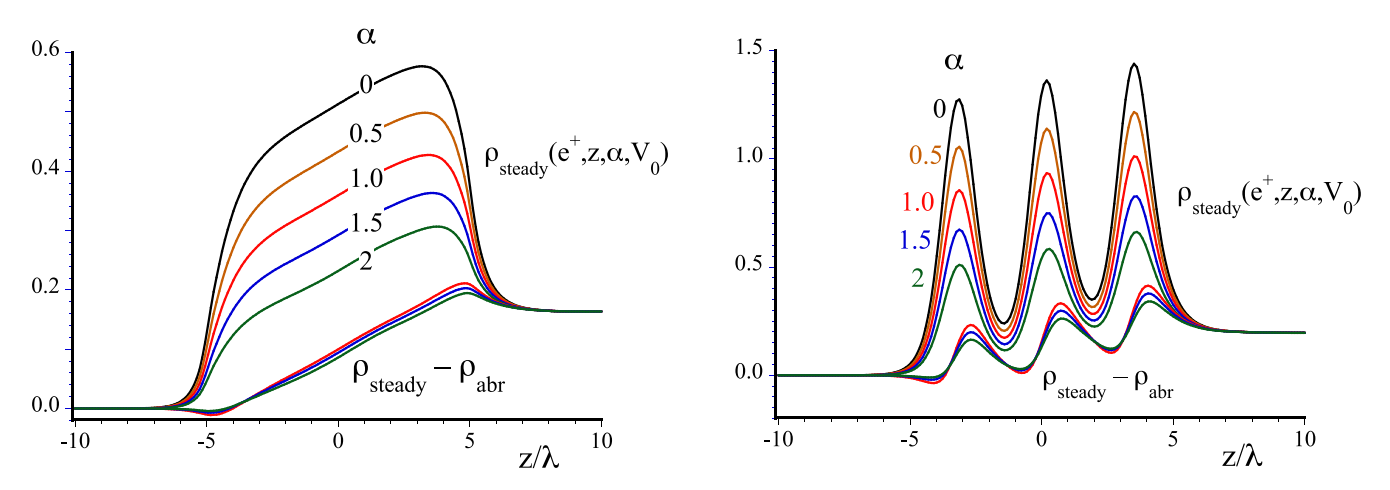


FIG. 4. The steady state of the positrons' spatial number density  $\rho_{steady}(e^+, z, \alpha, V_0)$  [according to the definition in Eq. (2.7)] for five values of the dressing parameter  $\alpha$  used in the projection operator and  $V_0 = 5$ . The bottom three curves are the difference  $\rho_{steady}(e^+, z, \alpha, V_0) - \rho_{abr}(e^+, z, \alpha, V_0)$  for  $\alpha = 1, 1.5$ , and 2. The final time t = 112.7 T. All other parameters as in Fig. 1, (a) for the constant electric field, (b) for the three-peaked electric field.

In fact, if we were to extrapolate these six curves to  $\alpha \to V_0$ , there should be almost no abruptons and  $N_{inside}(e^+, \alpha; V_0)$  should become the true number of created positrons inside the steady state for each value of  $V_0$ . For the special case of a simple quadratic polynomial match, i.e.,  $N_{inside}(e^+, \alpha; V_0) \approx a(V_0) + b(V_0)(\alpha - V_0) + c(V_0)(\alpha - V_0)^2$ , we found that the expansion factor  $c(V_0)$  was nearly independent of  $V_0$ , as it changed from 0.0011 (for  $V_0 = 2.5$ ) to 0.0010 (for  $V_0 = 5$ ) only rather insignificantly. To reiterate the findings from Sec. III B above, for  $-2 < \alpha < 2$  and  $-2 < V_0 < 2$  we found  $N_{inside}(e^+, \alpha; V_0) = 0.0011(\alpha - V_0)^2$ , where any population inside the interaction zone can be exclusively associated with abruptons. This finding is another independent

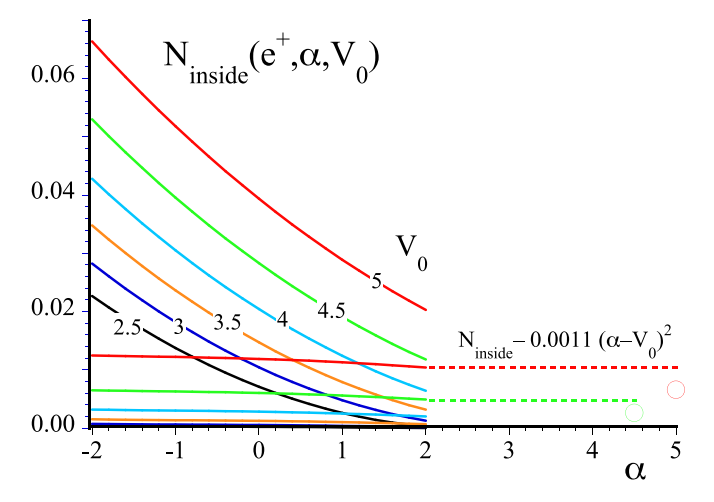


FIG. 5. The (uncorrected) number of positrons inside the interaction region according to  $N_{inside}(e^+,\alpha;V_0) \equiv \int dz \, \rho_{steady}(e^+,z;V_0,\alpha),$  where the spatial integration extends only from z=-d/2 to z=d/2. The two open circles (for  $V_0=5$  and 4.5) are the predictions from the extrapolated polynomials up to second order in  $(\alpha-V_0)$  and extrapolated to  $\alpha=V_0$ . The nearly horizonal straight lines [red (  $V_0=5$ ), green ( $V_0=4.5$ ), and blue ( $V_0=4.0$ ) ] are the corrected densities  $N_{inside}(e^+,\alpha;V_0){=}0.0011$  (  $V_0{=}\alpha)^2$  as a function of  $\alpha$ .

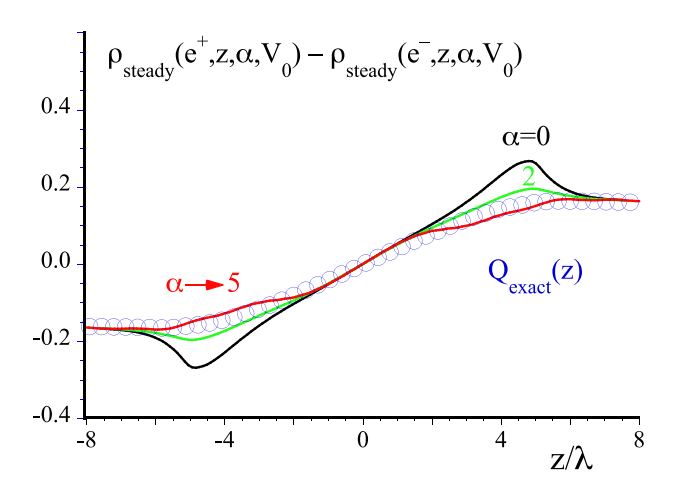
qualitative confirmation that the final positron populations inside the supercritical interaction zone differ mainly by abrupton-like contributions.

In Fig. 5 we have also graphed the corrected number of positrons, obtained by subtracting the abrupton-like contributions from the calculated quasipositron number, i.e.,  $N_{inside}(e^+,\alpha;V_0) - 0.0011(\alpha - V_0)^2$ . The resulting nearly horizontal lines show again that the  $\alpha$  dependence is again drastically reduced, suggesting that we can approximately associate this difference with the true number of physical positrons inside the supercritical interaction region.

### B. Comparison with the unambiguous electric current density

In our present understanding, the only physically observable quantity inside the supercritical interaction zone that can be calculated unambiguously without any projection is the total charge density  $Q_{\text{exact}}(z, t)$ , as it is defined from the full electron-positron field operator as  $Q_{\text{exact}}(z, t) \equiv e \langle \Psi^{\dagger}(z, t)\Psi(z, t)-\Psi(z, t)\Psi^{\dagger}(z, t)\rangle/2$ . We can therefore estimate the accuracy of our positronic density  $\rho_{\text{phys}}(e^+, z, t)$  defined in Eq. (3.1) by synthesizing the corresponding total charge density as  $Q_{\text{phys}}(z, t) \equiv \rho_{\text{phys}}(e^+, z, t) - \rho_{\text{phys}}(e^-, z, t)$ , where the electronic density could be obtained from a similar abrupton-subtraction approach. We note that a similar accuracy gauge was already presented in Refs. [24,25], where the accuracy of a machine learning-based algorithm to construct  $\rho_{\text{phys}}(e^+, z, t)$  and  $\rho_{\text{phys}}(e^-, z, t)$  was evaluated.

In Fig. 6 we present our results for the steady state for the constant and also three-peaked electric field case. The exact curve  $Q_{\rm exact}(z)$  that serves as an unambiguous yard-stick is presented by the blue open circles. We see that it increases rather monotonically from the left-hand side of the electric field (associated with ejected negatively charged electrons) to its right-hand side. The red curve was computed via  $\rho_{\rm steady}(e^+, z, \alpha) - \rho_{\rm steady}(e^-, z, \alpha)$  for  $\alpha = 0$  and  $V_0 = 5$ , as the contributions to the abruptons is identical here for the electrons and positrons, and prior subtraction of these terms from  $\rho_{\rm steady}$  would be irrelevant for the constructed



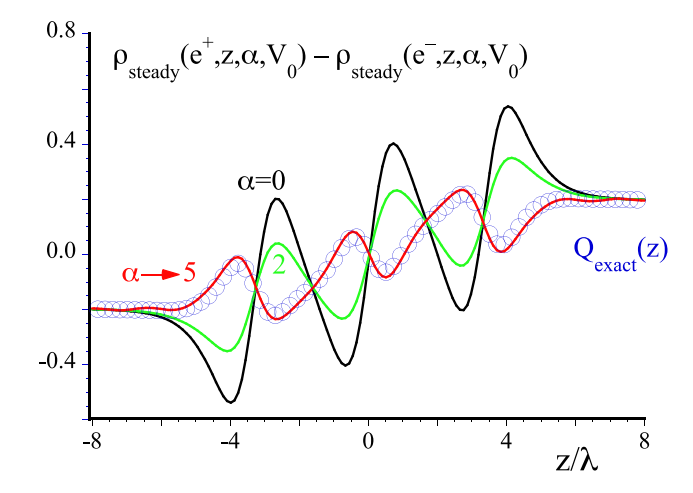


FIG. 6. Comparison of the steady-state total charge density  $Q_{exact}(z)$  defined in Sec. IV B and a constructed one based on the difference between the calculated positronic and electronic densities  $\rho_{phys}(e^+,z,\alpha,V_0)-\rho_{phys}(e^-,z,\alpha,V_0)$  for  $\alpha=0$  and  $\alpha=2$  for  $V_0=5$ . The red curve is the density  $\rho_{phys}(e^+)-\rho_{phys}(e^-)$  for  $\alpha=5$ , based on the extrapolated curves using  $\alpha=1.0,1.2,1.4,1,6,1.8$ , and 2.0. For comparison, the blue circles are the exact total charge density  $Q_{exact}(z)\equiv e\,\langle\Psi^\dagger\Psi-\Psi\Psi^\dagger\rangle/2$ . (a) For the constant electric field, and (b) for the three-peaked electric field.

total density. The red curve is the same difference, however, evaluated for  $\alpha=2$  and  $V_0=5$ . The red curve in the graph is based on extrapolating the six sets of densities  $\rho_{\text{steady}}(e^+, z, \alpha) - \rho_{\text{steady}}(e^-, z, \alpha)$  for  $\alpha=1, 1.2, 1.4, 1.6, 1.8,$  and 2.0 to  $\alpha=5$ . The agreement with the exact curve (open circles) is excellent and gives credence to the validity of this approach.

655

656

657

659

660

661

663

664

665

667

668

669

670

671

672

673

674

675

676

677

678

681

682

683

685

686

In order to perform this quantitative accuracy test also for more complicated electric field, we have repeated the same simulations for the three-peaked electric field defined at the top of Sec. III above. The corresponding data are shown in Fig. 6(b) and confirm the validity of our approach for a spatially inhomogeneous electric field.

### V. DISCUSSION AND FUTURE RESEARCH DIRECTIONS

In this study, we have explored an approach to derive accurate spatial densities of positrons created within the supercritical interaction zone. Our method involves subtracting projection-dependent corrections, aiming to uncover the true physical distribution of positrons. For scenarios involving subcritical external fields, these corrections can be unequivocally attributed to positrons termed abruptons, generated due to the abrupt changes in the potential's time dependence. We employed various numerical techniques, including long-time dynamics analysis, perturbation theory, and convolution-based integral expressions, to consistently evaluate these corrections. Subsequently, we applied these methods to the supercritical case, resulting in significant reductions in projectiondependent contributions. This subtraction-based approach serves as a theoretical means to investigate the actual spatial profile of physical positrons within the interaction region.

At this early stage of our research, numerous avenues for future investigation emerge. First and foremost, although we have primarily focused on one-dimensional dynamics for computational simplicity, there is no inherent obstacle to extending our methodology to three-dimensional systems. Additionally, even after the subtraction of the abrupton density, we observed a slight dependence on the chosen subspace for projection. Further exploration of techniques to minimize the remaining  $\alpha$ -dependent corrections is warranted. Currently, we lack a comprehensive interpretation of these remaining correction terms. Notably, the presence of existing physical positrons within the interaction zone appears to influence the spatial distribution of abruptons generated during abrupt potential turn offs. Here, the Pauli exclusion principle may play a pivotal role.

691

695

696

697

699

700

701

703

704

705

708

709

711

712

713

714

715

716

717

718

720

721

722

724

725

726

We have yet to conduct a comprehensive analysis of the accuracy of our approximate subtraction term across a broader range of V<sub>0</sub> or d values. Our primary emphasis has been on systematically varying the spatial profiles of the electric field while keeping  $V_0$  and d constant. Our investigation associated with transitions from constant to triply peaked field shapes indicates that the magnitude of the spatial gradient of the field does not necessarily compromise the quality of our subtraction term. As per definition, the subtraction term is exact for  $V_0 < 2mc^2$ , we anticipate a degradation in the quality of the subtraction term with increasing V<sub>0</sub>, a hypothesis consistent with our findings discussed in Sec. V. In that section, we observed that the presence of preexisting physical positrons within the interaction zone seems to impact the spatial distribution of abruptons generated during abrupt potential turn offs. In the same vein, we anticipate an improvement in accuracy for an increase in the extension parameter d (with a fixed  $V_0$ ) as the existing physical particles decrease.

Furthermore, our study has concentrated on the longtime steady-state distribution. However, it is conceivable to generalize our approach to address the short-time formation process. Once the potential stabilizes at a constant value, the abrupton-density's specific form should become independent of time, allowing for its subtraction from the time-dependent density.

An intriguing challenge also arises in defining a timedependent particle number when interacting with a rapidly oscillating external field. In addressing this issue, the locally constant field approximation (LCFA) [39,40] emerges as a

730

731

734

737

738

739

743

744

748

749

752

753

755

756

758

759

760

761

valuable tool. This method proves particularly beneficial in rendering complex space-time profiles of laser pulses accessible to theoretical approaches, such as the worldline instanton approach [41] or the quantum Vlasov equation [22,23,42]. Remarkably, the LCFA demonstrates great efficacy, especially when the wavelength of the laser surpasses the particles' formation length, and classical trajectories are localized near the field's maximum. This observation hints at the intriguing possibility that classical trajectory considerations could offer additional insights into the phenomenon.

Last, it is essential to acknowledge that our work relies on the framework of relativistic quantum field theory, which associates the field's coordinates with the actual particle positions. However, on a more fundamental level, unresolved conceptual questions persist regarding the relativistic localization problem and the correct choice for the position operator [36,43–48]. This issue is also partly linked to the fact that the continuum of upper energy states is incomplete, leading to the

impossibility of perfect spatial localization for any superposition within this subspace. This delocalization phenomenon was also considered in the convolution integral outlined in Eq. (3.6).

In summary, our study represents a further step towards understanding the true spatial distribution of positrons within supercritical interaction zones. However, numerous intriguing questions and promising research directions await exploration in the future.

### **ACKNOWLEDGMENTS**

C.G. would like to thank the ILP for its kind hospitality during his visit to Illinois State University. This work has been supported by the U.S. National Science Foundation and Research Corporation and the NSFC (No. 12304337). We also acknowledge generous access to the HPC supercomputer cluster provided by ISU.

- [1] Y. I. Salamin, S. X. Hu, K. Z. Hatsagortsyan, and C. H. Keitel, Relativistic high-power laser–matter interactions, Phys. Rep. 427, 41 (2006).
- [2] R. Ruffini, G. Vereshchagin, and S. S. Xue, Electron–positron pairs in physics and astrophysics: From heavy nuclei to black holes, Phys. Rep. 487, 1 (2010).
- [3] A. Di Piazza, C. Müller, K. Z. Hatsagortsyan, and C. H. Keitel, Extremely high-intensity laser interactions with fundamental quantum systems, Rev. Mod. Phys. 84, 1177 (2012).
- [4] B. S. Xie, Z. L. Li, and S. Tang, Electron-positron pair production in ultrastrong laser fields, Matter Radiat. Extremes 2, 225 (2017).
- [5] For an excellent review of the recent theoretical and experimental activities in strong-field QED, see the abstracts to the ExHilp 2019 conference at Stanford: https://web.stanford.edu/group/pulse\_institute/exhilp/exhilp2019\_program.pdf.
- [6] For a recent extensive review, see A. Fedotov, A. Ilderton, F. Karbstein, B. King, D. Seipt, H. Taya, and G. Torgrimsson, Advances in QED with intense background fields, Phys. Rep. 1010, 1 (2023).
- [7] S. Weinberg, *The Quantum Theory of Fields, Volume 1: Foundations* (Cambridge University Press, Cambridge, 1995).
- [8] M. E. Peskin and D. V. Schroeder, *An Introduction to Quantum Field Theory* (CRC Press, Boca Raton, 1995).
- [9] V. B. Berestetskii, E. M. Lifshitz, and L. P. Pitaevskii, *Relativistic Quantum Theory* (Pergamon Press, 1971).
- [10] M. Gavrila, Atoms in intense laser fields, *Adv. At., Mol. Opt. Phys*, Suppl. 1 (Academic Press, San Diego, 1992).
- [11] A. L'Huillier, K. J. Schafer, and K. C. Kulander, Theoretical aspects of intense field harmonic generation, J. Phys. B: At., Mol. Opt. Phys. **24**, 3315 (1991).
- [12] J. L. Krause, K. J. Schafer, and K. C. Kulander, High-order harmonic generation from atoms and ions in the high intensity regime, Phys. Rev. Lett. 68, 3535 (1992).
- [13] J. H. Eberly, J. Javavainen, and K. Rzazewski, Above-threshold ionization, Phys. Rep. 204, 331 (1991).
- [14] J. H. Eberly and K. C. Kulander, Atomic stabilization by superintense lasers, Science 262, 1229 (1993).

- [15] F. Sauter, On the behavior of an electron in a homogeneous electric field in Dirac's relativistic theory, Z. Phys. 69, 742 (1931).
- [16] J. Schwinger, On gauge invariance and vacuum polarization, Phys. Rev. 82, 664 (1951).
- [17] F. Gelis and N. Tanji, Schwinger mechanism revisited, Prog. Part. Nucl. Phys. 87, 1 (2016).
- [18] P. Krekora, Q. Su, and R. Grobe, Interpretational difficulties in quantum field theory, Phys. Rev. A 73, 022114 (2006).
- [19] C. C. Gerry, Q. Su, and R. Grobe, Timing of pair-production in time-dependent force fields, Phys. Rev. A **74**, 044103 (2006).
- [20] R. Dabrowski and G. V. Dunne, Superadiabatic particle number in Schwinger and de Sitter particle production, Phys. Rev. D 90, 025021 (2014).
- [21] R. Dabrowski and G. V. Dunne, On the time dependence of adiabatic particle number, Phys. Rev. D **94**, 065005 (2016).
- [22] J. Unger, S. Dong, R. Flores, Q. Su, and R. Grobe, Relationship of the pair creation yield during and after the interaction, Laser Phys. 29, 065302 (2019).
- [23] Y. Kluger, E. Mottola, and J. M. Eisenberg, The quantum Vlasov equation and its Markov limit, Phys. Rev. D **58**, 125015 (1998).
- [24] C. Gong, J. Bryan, Q. Su, and R. Grobe, Machine learning techniques in the examination of the electron-positron pair creation process, J. Opt. Soc. Am. B 38, 3582 (2021).
- [25] C. Gong, Q. Su, and R. Grobe, Birth process of electronpositron pairs inside supercritical fields, Eur. Phys. Lett. 141, 65001 (2023).
- [26] A. Ilderton, Physics of adiabatic particle number in the Schwinger effect, Phys. Rev. D 105, 016021 (2022).
- [27] M. Diez, R. Alkofer, and C. Kohlfürst, Identifying time scales in particle production from fields, Phys. Lett. B 844, 138063 (2023); See also M. Diez, Time-scales of particle formation in the Sauter-Schwinger effect, M.S. thesis, University of Graz, Graz, 2022.
- [28] See https://eli-laser.eu; I. C. E. Turcu *et al.*, Rom. Rep. Phys. **68**, S145 (2016).
- [29] See https://corels.ibs.re.kr.

- [30] For a nice project overview of the E-320 collaboration at FACET-II, (https://facet.slac.stanford.edu) see the conference slides by S. Meuren, https://conf.slac.stanford.edu/facet-2-2019/sites/facet-2-2019.conf.slac.stanford.edu/files/basicpage-docs/sfqed\_2019.pdf, presented at the FACET-II Science Workshop 2019 at SLAC.
- [31] C. H. Keitel, A. Di Piazza, G. G. Paulus, T. Stoehlker, E. L. Clark, S. Mangles, Z. Najmudin, K. Krushelnick, J. Schreiber, M. Borghesi, B. Dromey, M. Geissler, D. Riley, G. Sarri, and M. Zepf, Photo-induced pair production and strong field QED on Gemini, arXiv:2103.06059.
- [32] See <a href="http://www.hibef.eu">http://www.hibef.eu</a>; H. Abramowicz *et al.*, Conceptual design report for the LUXE experiment, Eur. Phys. J.: Spec. Top. 230, 2445 (2021).
- [33] W. Greiner, B. Müller, and J. Rafelski, *Quantum Electrodynamics of Strong Fields* (Springer, Berlin, 1985).
- [34] For a review, see T. Cheng, Q. Su, and R. Grobe, Introductory review on quantum field theory with space-time resolution, Contemp. Phys. **51**, 315 (2010).
- [35] P. Krekora, K. Cooley, Q. Su, and R. Grobe, Early time errants during the field-induced pair creation, Laser Phys. 16, 588 (2006).
- [36] P. Krekora, Q. Su, and R. Grobe, Relativistic electron localization and the lack of Zitterbewegung, Phys. Rev. Lett. 93, 043004 (2004).
- [37] F. Hund, Materieerzeugung im anschaulichen und im gequantelten Wellenbild der Materie, Z. Phys. 117, 1 (1941).
- [38] Q. Z. Lv, S. Dong, C. Lisowski, R. Pelphrey, Y. T. Li, Q. Su, and R. Grobe, Quantum mechanical approach to the laser-assisted vacuum decay, Phys. Rev. A **97**, 053416 (2018).

- [39] I. A. Aleksandrov, G. Plunien, and V. M. Shabaev, Locally-constant field approximation in studies of electron-positron pair production in strong external fields, Phys. Rev. D 99, 016020 (2019).
- [40] D. G. Sevostyanov, I. A. Aleksandrov, G. Plunien, and V. M. Shabaev, Total yield of electron-positron pairs produced from vacuum in strong electromagnetic fields: Validity of the locally constant field approximation, Phys. Rev. D 104, 076014 (2021).
- [41] G. V. Dunne, Q.-H. Wang, H. Gies, and C. Schubert, World-line instantons and the fluctuation prefactor, Phys. Rev. D 73, 065028 (2006).
- [42] F. Hebenstreit, R. Alkofer, and H. Gies, Pair production beyond the Schwinger formula in time-dependent electric fields, Phys. Rev. D **78**, 061701(R) (2008).
- [43] T. D. Newton and E. P. Wigner, Localized states for elementary systems, Rev. Mod. Phys. 21, 400 (1949).
- [44] M. H. L. Pryce, The mass-centre in the restricted theory of relativity and its connexion with the quantum theory of elementary particles, Proc. R. Soc. **195**, 62 (1948).
- [45] V. Bargmann and E. P. Wigner, Group theoretical discussion of relativistic wave equations, Proc. Natl. Acad. Sci. USA 34, 211 (1948).
- [46] T. Cheng, S. P. Bowen, C. C. Gerry, Q. Su, and R. Grobe, Locality in the creation of electron-positron pairs, Phys. Rev. A 77, 032106 (2008).
- [47] R. E. Wagner, M. R. Ware, E. V. Stefanovich, Q. Su, and R. Grobe, Local and non-local spatial densities in quantum field theory, Phys. Rev. A 85, 022121 (2012).
- [48] R. E. Wagner, B. T. Shields, M. R. Ware, Q. Su, and R. Grobe, Causality and relativistic localization in onedimensional Hamiltonians, Phys. Rev. A 83, 062106 (2011).